

LETTER TO THE EDITOR

Optical phonons in spin–Peierls compound NaV_2O_5

Z V Popović†, M J Konstantinović†, R Gajić†, V Popov‡, Y S Raptis§,
A N Vasil'ev||, M Isobe¶ and Y Ueda¶

† Institute of Physics, 11001 Belgrade, PO Box 57, Yugoslavia

‡ Faculty of Physics, University of Sofia, 1126 Sofia, Bulgaria

§ Physics Department, National Technical University, 15780 Athens, Greece

|| Low Temperature Department, Moscow State University, 119899 Moscow, Russia

¶ Institute for Solid State Physics, The University of Tokyo, Roppongi 7-22-1, Minato-ku, Tokyo 106, Japan

Received 12 May 1998

Abstract. We measured the room temperature far-infrared reflectivity and Raman scattering spectra of NaV_2O_5 single crystals. The frequencies of infrared active modes are obtained by Kramers–Kronig analysis of reflectivity data. The assignment of the observed modes is given according to the lattice dynamical calculation based on the valence shell model. According to the factor group analysis of the $P2_1mn$ space group, which assumes the existence of the V^{4+} and V^{5+} chains, the 15 A_1 and 7 B_1 modes can be expected in both ir and Raman scattering spectra from the (001) plane. Only eight Raman and six infrared modes of A_1 symmetry are clearly seen. In the case of B_1 symmetry, three B_1 modes are observed both in the Raman and in the ir reflectivity spectra. The frequencies of these ir and Raman modes differ significantly. Because of this, we concluded that the space group of the NaV_2O_5 crystal structure cannot be $P2_1mn$ (non-centrosymmetric), but the space group which includes the mutual exclusion between Raman and infrared activity (centrosymmetric space group). We have shown that the appropriate space group is $Pm\bar{m}n$, for which we found our experimental spectra in complete agreement with factor-group analysis. This means that V atoms are indistinguishable in the unit cell and in a mixed-valence state.

It has been shown recently [1] that sodium vanadium oxide is the second example of the inorganic spin–Peierls compound, following CuGeO_3 [2]. The spin–Peierls transition is one of the most interesting phenomena observed in low-dimensional quantum spin systems. It occurs in crystals containing linear chains of half integer spin coupled by an antiferromagnetic exchange interaction.

NaV_2O_5 , grown in single crystalline form under ambient conditions, has an orthorhombic unit cell [3] with parameters $a = 1.1318$ nm, $b = 0.3611$ nm, $c = 0.4797$ nm, $Z = 2$ and the space group $P2_1mn$ (D_{2v}^7). Such a crystalline structure assumes two kinds of vanadium chains along the b -axis. One is magnetic V^{4+} ($S = \frac{1}{2}$) and the other one is a nonmagnetic V^{5+} ($S = 0$) chains. Each vanadium atom is surrounded by five oxygen atoms, forming VO_5 pyramids. These pyramids are mutually connected via common edges to form layers in the (ab)-plane. The Na atoms are situated between these layers as intercalants. A schematic representation of the crystal structure of this oxide is given in figure 1.

Magnetic susceptibility measurements of NaV_2O_5 powder [1] show a broad maximum at 350 K, followed by rapid decrease below 34 K. Such susceptibility behaviour can be well described as a linear Heisenberg antiferromagnet in the high temperature phase and by Bulaevskii theory [4] in dimerized phase, indicating the true spin–Peierls transition at 34 K. Lattice dimerization and the opening of the spin–gap in NaV_2O_5 below the spin–Peierls

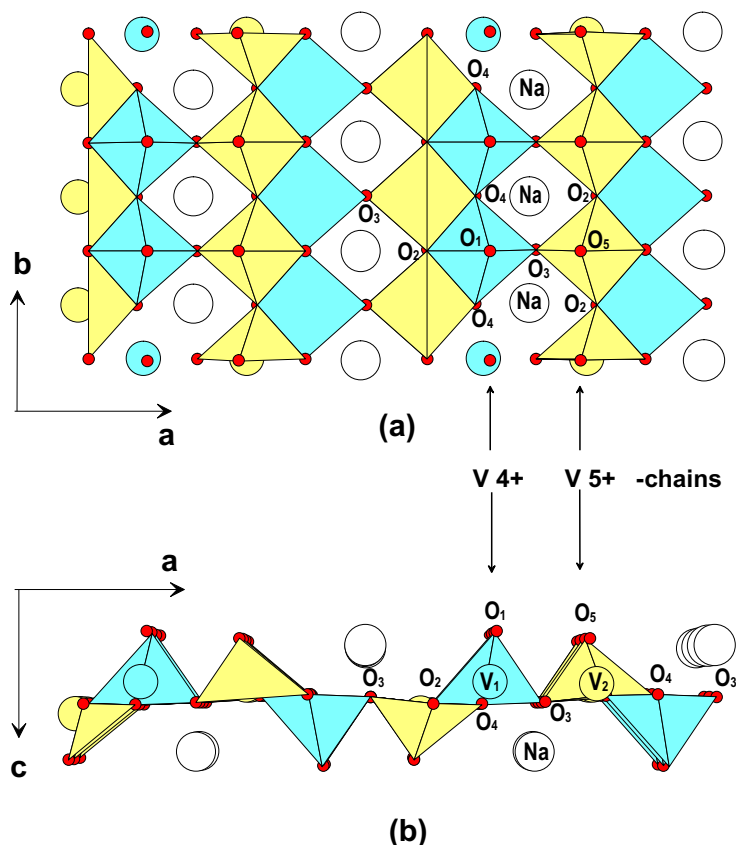


Figure 1. Schematic representation of the NaV₂O₅ crystal structure.

transition temperature have been observed in x-ray and neutron scattering measurements [5], nuclear magnetic resonance [6] and electron spin resonance [7] studies. Using these techniques [5–7], the spin-gap was estimated to be (98 ± 6) K.

Phonon properties of this oxide are poorly studied. The previous polarized infrared transmission [8, 9] and Raman scattering spectra [9, 10] of NaV₂O₅ above and below the spin–Peierls transition temperature reveal a crystallographic distortion at the transition temperature. No assignment of the observed modes was given. In our earlier paper [11] the polarized Raman scattering spectra were analysed in the spin–Peierls phase. It was shown that the one-magnon excitation and the onset of the magnetic continuum are at 66 cm^{-1} (93 K) and 132 cm^{-1} (186 K), in good agreement with previous estimation of the spin-gap.

The present work was performed using single crystals grown from the melt, using the self-flux method [12]. Crystals were plates with dimensions typically about $1 \times 3 \times 0.5 \text{ mm}^3$ in the *a*, *b* and *c* axes, respectively. For optical measurements we used (001)- oriented samples. The infrared measurements were carried out with a BOMEM DA-8 FTIR spectrometer. A DTGS pyroelectric detector was used to cover the wave number region from 100 to 700 cm^{-1} and a cooled HgCdTe detector was used from 500 to 6000 cm^{-1} . The Raman spectra were measured in the backscattering configuration using a

micro-Raman system with a Jobin Yvon 64000 triple monochromator including a nitrogen-cooled CCD-detector. An Ar-ion laser was used as the exciting source.

As previously mentioned, the NaV₂O₅ unit cell consists of two formula units comprising 16 atoms in all. Because all atoms in the unit cell have the same site symmetry (C_s) the factor group analysis yields

$$(\text{V, Na, O}_1, \text{O}_2, \text{O}_3, \text{O}_4, \text{O}_5)(\text{C}_s) \quad \Gamma = 2A_1 + A_2 + B_1 + 2B_2. \quad (1)$$

Summarizing the representations given above and subtracting acoustic ($A_1 + B_1 + B_2$) modes, we obtain the irreducible representations of NaV₂O₅ vibrational modes

$$\Gamma_{opt} = 15A_1(\mathbf{E} \parallel a, aa, bb, cc) + 8A_2(bc) + 7B_1(\mathbf{E} \parallel b, ab) + 15B_2(\mathbf{E} \parallel c, ac). \quad (2)$$

Since the A_1 , B_1 and B_2 mode are infrared active (for $\mathbf{E} \parallel a$, $\mathbf{E} \parallel b$ and $\mathbf{E} \parallel c$, respectively), 37 infrared frequencies are permitted. All 45 optical modes are to be expected in the NaV₂O₅ Raman spectra.

Room temperature polarized far-infrared reflectivity spectra of NaV₂O₅, in the spectral range from 125 to 1000 cm⁻¹, are given in lower part of figure 2. In the case of $\mathbf{E} \parallel a$ polarization three continuum features at about 3500 (inset of figure 2), 530 and 280 cm⁻¹ are seen. These structures are depicted by the 'shadow region' in figure 2. Besides these continua, six oscillators with TO energies at 140, 254, 436, 469, 505 and 940 cm⁻¹ are observed. While the 280 and 3500 cm⁻¹ continua are clearly seen in figure 2, the presence of the 530 continuum is manifested through the quite uncharacteristic oscillator shape of the dominant structure between 500 and 620 cm⁻¹. Similar continua are observed in room temperature Raman spectra (figure 2) and we will discuss them later on. For $\mathbf{E} \parallel b$ polarization only three oscillators at about 177, 372 and 582 cm⁻¹ are clearly observed. The TO and LO frequencies of observed ir-active modes, obtained using Kramers–Kronig analysis of reflectivity data, are collected in tables 1 and 2.

The room temperature Raman spectra of NaV₂O₅ for parallel and crossed polarization are given in upper part of figure 2. The spectra for parallel polarizations consist of A_1 symmetry modes. Seven modes at 90, 179, 306, 424, 452, 536 and 969 cm⁻¹ are clearly seen for the (aa) polarization and one additional mode at 234 cm⁻¹ for the (bb) polarization. For crossed polarization only three Raman active modes at 175, 297 and 684 cm⁻¹ are observed.

The calculation of the Γ -phonons of NaV₂O₅ was carried out within a valence shell model (VSM). The model parameters were taken over from V₂O₅ for which infrared and Raman data exist. A previous extensive study of the lattice dynamics of V₂O₅ was accomplished using VFF [13]. However, this model could not be used in the case of NaV₂O₅ because Na–O interactions are predominantly ionic and require the introduction of ionic charges. For this reason, the VSM was adopted and the model parameters were fitted to the available infrared and Raman data for V₂O₅. Supplementary to the bond-stretching and angle-bending interactions, a weak Van der Waals attraction was accepted for the O–O interactions. The deformation of the electron density of the atoms was accounted for in dipole approximation by using shell charges and ionic polarizabilities. The phonon frequencies for V₂O₅ calculated with the best fit model parameters [14] are shown in tables 1 and 2. In all cases the agreement with the experimental data is good except for the ir-active modes observed at 303 and 411 cm⁻¹, where the calculated TO frequencies are 70–80 cm⁻¹ higher. The model parameters for V₂O₅ were transferred to NaV₂O₅ where the Na and Na–O parameters were obtained by additional fitting to two phonons observed in the Raman spectra at 969 cm⁻¹ (A_1) and 684 cm⁻¹ (B_1). The calculated phonons in NaV₂O₅ are compared to the observed lines in the Raman spectra in tables 1 and 2. Besides

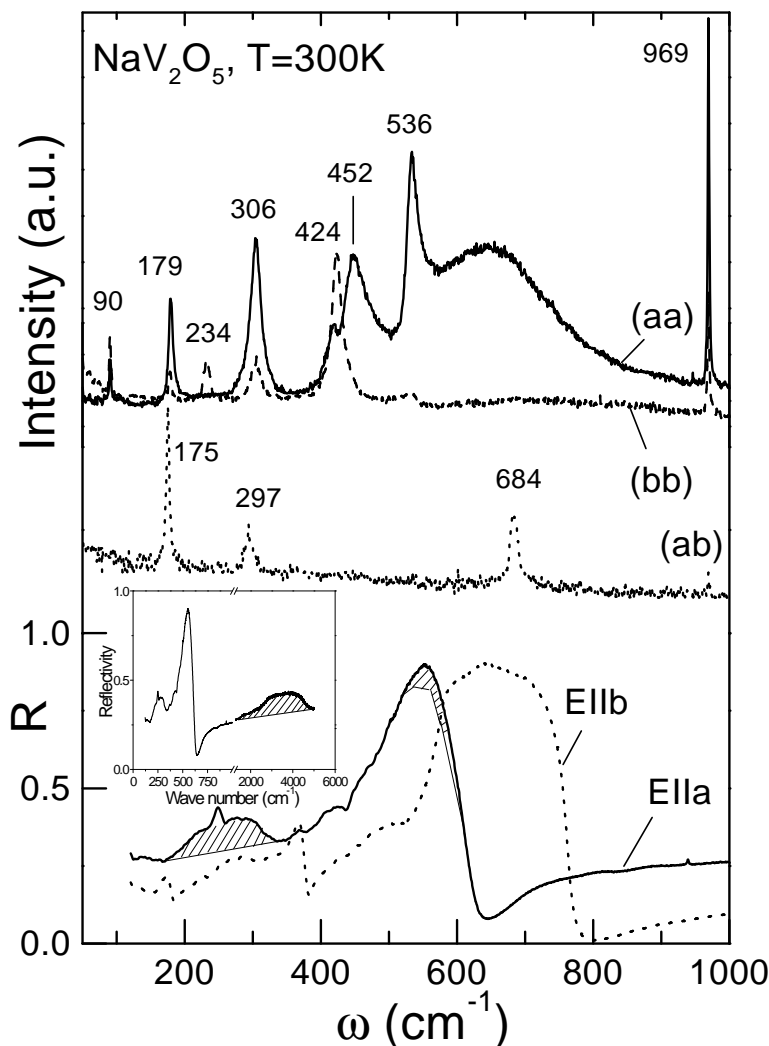


Figure 2. Room temperature polarized far-infrared reflectivity spectra of NaV_2O_5 single crystal in the 125–1000 cm^{-1} spectral range for the $E \parallel a$ (A_1 modes) and $E \parallel b$ (B_1 modes) polarizations (below). Raman scattering spectra at room temperature for different polarization configurations (above).

the one-to-one correspondence of most of the modes in NaV_2O_5 to those in V_2O_5 , there are phonons which mainly involve motion of Na. There are four modes of A_1 symmetry (164 and 186 cm^{-1}) and B_2 symmetry (176 and 188 cm^{-1}) in which Na atoms move in the ac -plane and two modes with symmetry A_2 (349 cm^{-1}) and B_1 (347 cm^{-1}) with displacement of Na atoms along the c -axis. The measured Raman spectrum allows us to assign the peak at 179 cm^{-1} observed in the (aa) configuration to one of the mentioned A_1 modes.

According to lattice dynamical calculation, the highest energy phonon modes correspond to stretching vibrations of the shortest bonds, in this case $\text{V}_{1(2)}\text{--O}_{1(5)}$. These modes are observed in ir and Raman spectra at 940 and 969 cm^{-1} respectively, in agreement with the

Table 1. Experimental and calculated frequencies of the $A_1\Gamma$ -point phonons in NaV_2O_5 and comparison with the Γ -point phonons in V_2O_5 . The following notation is used: O stands for O_2 and O_4 , O_{ap} for O_1 and O_5 and O_b for O_3 . In O–V–O the symbol O denotes any oxygen atom.

| Mode | NaV_2O_5 | | | Remarks | V_2O_5 | | | |
|-------|--------------------------|---------|---------|-------------------------------|------------------------|---------|---------|-------|
| | Exp. | | Calc. | | Mode | Exp. | | Calc. |
| | Raman | ir | | | | Mode | Exp. | |
| A_1 | — | — | 100/103 | Chain transl. c | B_{3u} | 72/76 | 103/109 | |
| | 90 | — | 105/105 | Chain transl. c | A_{1g} | 107 | 103 | |
| | — | 140/146 | 164/170 | Na c | — | — | — | |
| | 179 | — | 186/188 | Na a | — | — | — | |
| | 234 | — | 254/256 | O–V–O bending | A_{1g} | 200 | 218 | |
| | — | 254/258 | 273/273 | O–V–O bending | B_{3u} | 261/266 | 266/267 | |
| | 306 | — | 311/311 | O–V–O bending | A_{1g} | 310 | 295 | |
| | 424 | — | 364/368 | O–V–O bending | B_{3u} | 360/391 | 362/366 | |
| | — | 436/438 | 400/400 | O–V–O bending | A_{1g} | 404 | 405 | |
| | 452 | — | 475/475 | V–O stretching | A_{1g} | 483 | 486 | |
| | — | 469/472 | 479/479 | V–O stretching | B_{3u} | 460/586 | 489/489 | |
| | 536 | — | 531/531 | V– O_b –V bending | A_{1g} | 528 | 529 | |
| | — | 505/625 | 699/777 | V– O_b stretching | B_{3u} | 768/959 | 761/793 | |
| | — | 940/941 | 949/950 | V– O_{ap} stretching | A_{1g} | 992 | 988 | |
| | 969 | — | 973/985 | V– O_{ap} stretching | B_{3u} | 981/982 | 983/993 | |

Table 2. Experimental and calculated frequencies of the $B_1\Gamma$ -point phonons in NaV_2O_5 and comparison with the Γ -point phonons in V_2O_5 .

| Mode | NaV_2O_5 | | | Remarks | V_2O_5 | | | |
|-------|--------------------------|---------|---------|------------------------|------------------------|---------|---------|-------|
| | Exp. | | Calc. | | Mode | Exp. | | Calc. |
| | Raman | ir | | | | Mode | Exp. | |
| B_1 | 175 | — | 176/177 | Chain transl. | B_{1g} | 147 | 167 | |
| | — | 177/185 | 202/205 | O–V–O bending + Na b | B_{2u} | 212/225 | 225/225 | |
| | — | — | 273/274 | O–V–O bending | B_{2u} | 284/313 | 251/357 | |
| | 297 | — | 285/286 | O–V–O bending | B_{1g} | 290 | 286 | |
| | — | 372/380 | 347/352 | Na b | — | — | — | |
| | — | 582/765 | 487/497 | V–O stretching | B_{2u} | 507/843 | 523/820 | |
| | 684 | — | 681/692 | V–O stretching | B_{1g} | 702 | 706 | |

calculated values (table 1). The stretching V– O_3 vibrational mode, expected at 699 cm^{-1} (table 1), is not observed in our spectra. It is interesting to note that the Raman mode at 536 cm^{-1} originates from V– O_3 –V bending vibrations. This mode shows a strong asymmetry due to coupling with the electron background which peaked at 640 cm^{-1} . The similar broad continua are observed in both ir and Raman spectra, concerning their energies. These continua and phonons with their energies overlapping each other are analysed on the basis of resonance effects. It is found [11] that such phonons exhibit Fano asymmetry that can be associated with a strong absorption line at 1.25 eV, observed in absorption measurement [9]. The asymmetry is observed for 254 and 505 cm^{-1} ir active phonons in $E \parallel a$ spectra, where continuum-like features are observed. Because of that and similarities between continua energies in ir and Raman spectra we suggest that they have the same origin

| $P2_1mn$ Activity | | $Pm\bar{m}n$ Activity | |
|-------------------|-------------------------|---------------------------|------------------|
| $15A_1$ | R(aa,bb,cc) ir(Ella) | $8A_g$ | R(aa,bb,cc) |
| | | $7B_{3u}$ | ir(Ella) |
| $8A_2$ | R(bc) | $3A_u$ | silent |
| | | $5B_{3g}$ | R(bc) |
| $7B_1$ | R(ab) ir(Ellb) | $3B_{1g}$ | R(ab) |
| | | $4B_{2u}$ | ir(Ellb) |
| $15B_2$ | R(ac) ir(Ellc) | $7B_{1u}$ | ir(Ellc) |
| | | $8B_{2g}$ | R(ac) |
| $1A_1+1B_1+1B_2$ | | $1B_{1u}+1B_{2u}+1B_{3u}$ | Acoustic phonons |

Figure 3. The compatibility diagram relating the vibrations of modes of NaV₂O₅ in the $P2_1mn$ and $Pm\bar{m}n$ space groups.

and correspond to d–d electron transitions in vanadium ions. Furthermore, the A_1 modes with energies around 500 cm⁻¹ in the spectra correspond to V₁₍₂₎–O₂₍₄₎ vibrations. The modes in the 200–400 cm⁻¹ energy range can be described as O–V–O bending vibrations. As a possible phonon mode arising from the sodium vibrations, we suggest the 179 cm⁻¹ mode.

Let us again discuss the crystal symmetry and phonon selection rules. From 15 A_1 and 7 B_1 predicted by FGA, only eight (aa) and (bb) polarized modes and 3 (ab) polarized modes are clearly seen in the Raman spectra. In the infrared spectra only 6 $E \parallel a$ and 3 $E \parallel b$ modes are found and with completely different energies than Raman-active modes (tables 1 and 2). Accordingly, we concluded that the space group of NaV₂O₅ cannot be $P2_1mn$ (non-centrosymmetric) but the space group which includes mutual exclusion between Raman and infrared activity, the centrosymmetric group. Because of the strong anisotropy in the ab -plane, the space group must be orthorhombic. From all orthorhombic point groups only the D_{2h} group has the centre of symmetry. In the $P2_1mn$ space group, the four factor-group operators are: 1—the identity; 2₁—the twofold screw axis parallel to the a axis; m —the mirror plane perpendicular to the b axis and n —the glide plane perpendicular to the c axis with a glide translation ($a/2 + b/2$). In order to obtain the centrosymmetric space group it is necessary to introduce a mirror plane perpendicular to the a axis. In this case we obtained the $Pm\bar{m}n$ space group as the most probable space group of NaV₂O₅. This space group has the same general conditions [15] for possible reflections as $P2_1mn$ and no extra hkl conditions for atoms with C_s and C_{2v} site symmetry. The introduction of a mirror plane perpendicular to the a axis produces no different sites of V₁₍₂₎, O₁₍₅₎ and O₂₍₄₎ ions (see figure 1). The site symmetries of Na and O₃ ions in the $Pm\bar{m}n$ space group should be C_{2v} , and of V₁₍₂₎, O₁₍₅₎, O₂₍₄₎ ions should be C_s . The FGA of the new space group yields [16]

$$C_s(V_{1(2)}, O_{1(5)}, O_{2(4)}) \quad \Gamma = 2A_g + A_u + B_{1g} + 2B_{1u} + 2B_{2g} + B_{2u} + B_{3g} + 2B_{3u}$$

$$C_{2v}(Na, O_3) \quad \Gamma = A_g + B_{1u} + B_{2g} + B_{2u} + B_{3g} + B_{3u}.$$

Summarizing these representations and subtracting acoustic ($B_{1u} + B_{2u} + B_{3u}$) and silent ($3A_u$) modes, we obtained the irreducible representations of NaV₂O₅ vibrational modes of

the $Pm\bar{m}n$ space group:

$$\Gamma = 8A_g(aa, bb, cc) + 3B_{1g}(ab) + 8B_{2g}(ac) + 5B_{3g}(bc) + 7B_{1u}(E \parallel c) + 4B_{2u}(E \parallel b) + 7B_{3u}(E \parallel a). \quad (3)$$

The compatibility diagram relating the vibrational modes of NaV_2O_5 in the $P2_1mn$ and $Pm\bar{m}n$ space groups is given in figure 3. Our experimental spectra are in complete agreement with the FGA prediction for the $Pm\bar{m}n$ space group. Namely, FGA (equation (2)) predicts 8 A_g and 3 B_{1g} modes, as we experimentally observed in figure 2. In the case of ir modes we found six B_{3u} and three B_{2u} modes, in very good agreement with equation (2).

In conclusion, the appearance of infrared and Raman active modes at different frequencies, and the fact that the number of experimentally observed modes is in complete agreement with the FGA prediction for the $Pm\bar{m}n$ space group, support our findings that the crystal structure of NaV_2O_5 consists of edge and corner sharing VO_5 pyramids with no different vanadium and oxygen atoms. This structure could be isostructural with CaV_2O_5 [17].

This work was supported by the Serbian Ministry of Science and Technology under Project No 01E09.

References

- [1] Isobe M and Ueda Y 1996 *J. Phys. Soc. Japan* **65** 1178
- [2] Hase M, Terasaki I and Uchinokura K 1993 *Phys. Rev. Lett.* **70** 3651
- [3] Carpy A and Galy J 1975 *Acta Crystallogr. B* **31** 1481
- [4] Bulaevskii L N, Buzdin A I and Khomskii D I 1978 *Solid State Commun.* **27** 5
- [5] Fujii Y, Nakao H, Yosihama T, Nishi M, Nakajima K, Kakurai K, Isobe M, Ueda Y and Sawa H 1997 *J. Phys. Soc. Japan* **66** 326
- [6] Ohama T, Isobe M, Yasuoka H and Ueda Y 1977 *J. Phys. Soc. Japan* **66** 545
- [7] Vasil'ev A N, Smirnov A I, Isobe M and Ueda Y 1977 *Phys. Rev. B* **56** 5065
- [8] Popova M N, Sushkov A B, Vasil'ev A N, Smirnov A I, Isobe M and Ueda Y 1977 *Pis'ma Zh. Eksp. Teor. Fiz.* **65** 711 (Engl. transl. 1977 *JETP Lett.* **65** 743)
- [9] Golubchik S A, Isobe M, Ivlev A N, Mavrin B N, Popova M N, Sushkov A B, Vasil'ev A N and Ueda Y 1977 *J. Phys. Soc. Japan* **66** 4042
- [10] Weiden M, Hauptmann R, Geibel C, Steglich F, Fischer M, Lemmens P and Guntherodt G 1997 *Z. Phys. B* **103** 1
- [11] Konstantinovic M J, Popovic Z V, Vasil'ev A N, Isobe M and Ueda Y 1998 unpublished
- [12] Isobe M, Kagami C and Ueda Y *J. Cryst. Growth* at press
- [13] Clauws P, Broeckx J and Vennik J 1985 *Phys. Status Solidi b* **131** 459
- [14] Popov V 1998 unpublished
- [15] 1969 *International Tables for X-ray Crystallography* vol I, 3rd edn (Birmingham: Kynoch)
- [16] Rousseau D L, Bauman R P and Porto S P S 1981 *J. Raman Spectrosc.* **10** 253
- [17] Onoda M and Nishiguchi N 1996 *J. Solid State Chem.* **127** 359